A Numerical Study on Invariant Manifold Related to Transition of Intrinsic Localized Mode in Coupled Cantilever Array

Masayuki Kimura[†] and Takashi Hikihara[†]

†Department of Electrical Engineering, Kyoto University
Katsura, Nishikyo, Kyoto 615-8510 Japan
Email: kimura@dove.kuee.kyoto-u.ac.jp, hikihara@kuee.kyoto-u.ac.jp

Abstract—Intrinsic localized mode (ILM) is spatially localized and temporally periodic oscillation in nonlinear coupled oscillators. Recently, ILM has been observed in a micro-cantilever array by Sato *et al*. We deal with the dynamical properties of ILM in a homogeneous cantilever array with fixed boundaries. The coexistence and the stability of ILMs are investigated. The stability of ILM is changed with the nonlinear inter-site potential when the nonlinear on-site potential is fixed. The ILMs can exchange their stability between stable mode and unstable mode depending on the nonlinear inter-site potential. The transition is discussed based on the invariant manifold related to an unstable ILM. It is clarified that localized oscillations due to a stable ILM can shift their position via the stability change of ILM.

1. Introduction

Intrinsic localized mode (ILM) is spatially localized and temporally periodic solution in a nonlinear coupled oscillators. The localized solution is also called as discrete breather (DB). Tremendous number of analytical and numerical studies have been reported since the discovery of ILM by Sievers and Takeno [1]. In this decade, experimental investigations have been also reported. ILM is generated and observed in various systems, for instance, Josephson-junction array [2, 3, 4], optic wave guides [5, 6], micromechanical oscillators [7], and so on. They provide us the generality of phenomena and the possibility of applications as a localized exciter. Indeed, the studies toward future applications are increasing both in fundamental science and in practical engineering [8].

ILM in a micro-cantilever array was observed by Sato *et al.* [7, 9]. The micro-cantilever array was fabricated by microelectromechanical system (MEMS) technology. A piezo-electric vibrator was attached to substrate of the array. The frequency of vibration was chirped enough to excite ILMs. They observed not only pinned ILMs but also moving ILMs. The moving ILMs appeared while chirping the excitation. Some moving ILMs were pinned after the chirping was stopped. In addition, it was experimentally confirmed that the position of ILM can be shifted by creating a local defect [10, 11]. These results directly suggest that ILM can apply to MEMS applications in practical engineering. For applications, it will be a clue to understand the mechanism of moving ILM.
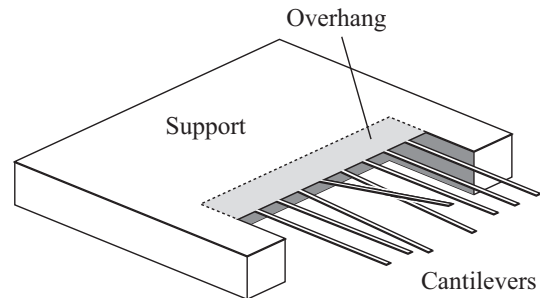

Figure 1: Schematic configuration of cantilever array. Eight homogeneous cantilevers are arranged at equal intervals. Each cantilever is coupled to its neighbors by overhang part. Both ends of array are fixed.

The moving ILM is considered as a wave propagation, phenomenologically. Propagation of a traveling wave was investigated in a coupled magneto-elastic beam system [12, 13, 14], in which each short beam oscillates under nonlinear magnetic potential. The long elastic beam connects these oscillators in one dimension. An external exciter is linked to one of the ends of oscillators array through coupling beam. The other end is kept free. Many stable and unstable standing waves coexist in the system. It is shown that there are heteroclinic connections of stable and unstable manifolds of unstable standing waves. Propagation of the traveling wave is governed by the invariant manifolds of unstable standing waves [14]. The moving ILM also seems to be governed by invariant manifolds of unstable pinned ILMs.

This paper examines the stability and the transition of ILM. The coexistence of ILMs is confirmed and the stability is investigated in Sec. 3. Invariant manifolds of the unstable ILM are numerically obtained in Sec. 4. In addition, the transition of ILM is also discussed with respect to stability change.

2. Coupled Cantilever Array

A cantilever array considered in this paper is shown in Fig.1. For simplicity, we deal with the mono-element cantilever array. Eight homogeneous cantilevers are equally spaced in one dimension. The overhang part couples adja-
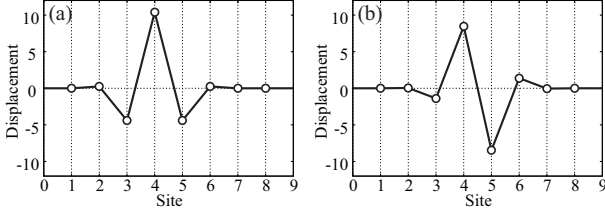
Figure 2: Coexisting ILMs in the cantilever array at $\alpha = 0.1, \beta_1 = 0.01, \beta_2 = 0.005$. (a) Sievers-Takeno (ST) mode centered on 4th cantilever. (b) Page (P) mode centered between 4th and 5th cantilevers. Each circle indicates the position of cantilever tip and each line between circles is the schematic coupling connection. We applied Newton-Raphson method to obtain these ILMs, and the 4th-order Runge-Kutta method to integrate Eq.(1). The accuracy of the numerical simulation is confirmed through the conservation of Hamiltonian H. Numerical error is kept under ϵH. In this paper, $H = 250$ and $\epsilon = 10^{-12}$.

Figure 3: Floquet multipliers λ in complex plane for P3-4. In left panel (a), all Floquet multipliers are represented. Near +1 in complex plane is shown in right panel (b). Dotted line corresponds to unit circle. Circle and square indicate Floquet multipliers for P3-4 at $\beta_2 = 5.452 \times 10^{-3}$ and $\beta_2 = 5.455 \times 10^{-3}$, respectively. Since a Floquet multiplier is outside unit circle, P3-4 is unstable at $\beta_2 = 5.452 \times 10^{-3}$. In contrast, P3-4 is stable when β_2 increases slightly. All Floquet multipliers are on unit circle.

cent cantilevers. Both ends of the array are fixed by the support. The motion of cantilevers are governed by the Euler-Bernoulli beam equation when the dumping can be neglected. The vibration of the tip of cantilever is described by the coupled non-dimensional ordinary differential equations as follows:

$$
\begin{aligned}
\ddot{u}_i = & -u_i - \beta_1 u_i^3 \\
& -\alpha (u_i - u_{i-1}) - \alpha (u_i - u_{i+1}) \\
& -\beta_2 (u_i - u_{i-1})^3 - \beta_2 (u_i - u_{i+1})^3, \\
& i \in \{1, 2, \ldots, 8\},
\end{aligned} \tag{1}
$$

where u_i denotes the displacement of the tip of i-th cantilever from equilibrium position. α depicts the ratio in quadratic potentials. The quartic potential coefficients are represented by β_1 and β_2. β_1 denotes the on-site one and it is set at 0.01 through this paper. The boundary conditions are set for given fixed-ends; $u_0 = u_9 = 0$, $\dot{u}_0 = \dot{u}_9 = 0$. The Hamiltonian

$$
\begin{aligned}
H = & \sum_i \left\{ \frac{1}{2} \dot{u}_i^2 + \frac{1}{2} u_i^2 + \frac{\beta_1}{4} u_i^4 \right. \\
& \left. + \frac{\alpha}{2} (u_i - u_{i-1})^2 + \frac{\beta_2}{4} (u_i - u_{i-1})^4 \right\}
\end{aligned} \tag{2}
$$

gives the total energy of the cantilever array. The array keeps the energy given by the initial condition during the temporal development.

3. Coexistence and Stability of ILM

Several ILMs coexist in the coupled cantilever array at the total energy $H = 250$. Two of the ILMs are shown in Fig.2. They are obtained by Newton-Raphson method with appropriate initial conditions. In general, coexisting ILMs are roughly classified into two kinds, "Sievers-Takeno mode (ST-mode)" and "Page mode (P-mode)" [15].
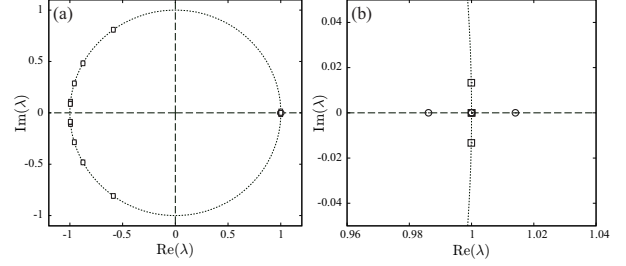
The ST-mode shown in Fig.2 has symmetric amplitude distribution in space and it is centered on a site. It was found analytically by Sievers and Takeno [1]. On the other hand, the P-mode, which was analytically derived in 1990 [16], is spatially antisymmetric and centered between sites. In the cantilever array, both ST- and P-modes can coexist at every site except near edges. Here we distinguish them by index number of cantilever at which the center of each ILM stands. For example, ST4 implies the ST-mode centered on the 4th cantilever and P4-5 implies the P-mode centered between the 4th and the 5th cantilevers.

As for the confirmation of the stability of ILMs, Floquet theory plays a main role [17]. ILM becomes unstable when one of the Floquet multipliers at least exists outside unit circle in complex plane. ILM is determined as marginally stable in the case that all Floquet multipliers are on the unit circle. Fig. 3 shows Floquet multipliers for P3-4 in two cases. The case of $\beta_2 = 5.452 \times 10^{-3}$ is represented by circles. Fig. 3(b) clearly shows that P3-4 is unstable. On the other hand, P3-4 becomes stable when $\beta_2 = 5.455 \times 10^{-3}$. All Floquet multipliers are on unit circle, which are indicated by squares in Fig.3. The stability of another coexisting P-modes near center of the array is also different between $\beta_2 = 5.452 \times 10^{-3}$ and 5.455×10^{-3}. Thus the stability of P-modes is changed by varying β_2 without significant change of the period and the amplitude distribution. For coexisting ST-modes, the stability change also occurs but the stability of ST-modes is opposite to P-modes. It suggests that the stability of ILMs is substantially affected by β_2.

4. ILM Transition via Stability Change

Based on results in the coupled magneto-elastic beam system [14], dynamics of moving ILM in the cantilever array is governed by invariant manifold of unstable ILMs. In this paper, the unstable manifold of P3-4 is focused on. The

P3-4 is unstable when $\beta_2 = 5.452 \times 10^{-3}$. One of Floquet multipliers is outside unit circle in complex plane as shown in Fig.3(b). Thus P3-4 has one dimensional unstable manifold. Since another Floquet multiplier is inside unit circle, P3-4 also has one dimensional stable manifold.

A nonlinear map $\mathcal{F}$ is defined on a hyper plane Σ_4 to obtain the unstable manifold of ILM. The hyper plane is defined as follows,

$$\Sigma_4 = \left\{ (u_1, \ldots, u_8, \dot{u}_1, \ldots, \dot{u}_8) \in \mathbf{R}^{16} \mid u_4 > 0, \dot{u}_4 = 0 \right\}. \quad (3)$$

As a result, the coexisting ILMs are represented as fixed points under the map $\mathcal{F} : \Sigma_4 \to \Sigma_4$. The unstable manifold of P3-4 projected onto a subspace of Σ_4 is shown in Fig.4. Solid curve corresponds to the unstable manifold $W^{\mathrm{u}}_{\mathrm{P3-4}}$ from P3-4. Coexisting ST-modes and P-modes are indicated by circles and squares. The unstable manifold of right side in Fig.4 extends to P5-6 and returns back to P3-4 again. The unstable manifold passes near P4-5 and P5-6 and takes a long way around ST4 and ST5. The fact suggests that a localized oscillation generated from a initial condition near P3-4 can move to near P4-5 and P5-6 [14]. However, the localized oscillation cannot reach near any ST-modes. It allows us to expect that a localized oscillation near stable ST-modes stays there for a long period. Hence the moving localized oscillation will stop near P4-5 or P5-6 which are stabilized by slightly increasing β_2.

The energy distribution in the cantilever array is defined so as to discuss moving localized oscillation as follows,

$$
\begin{aligned}
E(s, t) &= \begin{cases} E_{\mathrm{C}}(i, t) & (s = i), \\ E_{\mathrm{O}}(i, t) & (s = i - \frac{1}{2}), \end{cases} \quad (4) \\
&\quad s \in \left\{ \frac{1}{2}, 1, \frac{3}{2}, 2, \cdots, 8, \frac{17}{2} \right\}, \\
E_{\mathrm{C}}(i, t) &= \frac{1}{2}\dot{u}_i^2 + \frac{1}{2}u_i^2 + \frac{\beta_1}{4}u_i^4, \\
E_{\mathrm{O}}(i, t) &= \frac{\alpha}{2}(u_i - u_{i-1})^2 + \frac{\beta_2}{4}(u_i - u_{i-1})^4.
\end{aligned}
$$

Here, s depicts coordinate in space. $E_{\mathrm{C}}(i, t)$ denotes the sum of kinetic energy and potential energy of i-th cantilever tip. Potential energy of the overhang part between i-th and $(i-1)$-th cantilevers is represented as $E_{\mathrm{O}}(i, t)$.

Numerical simulation of catch and release manipulation for localized oscillation is shown in Fig.5. At first, β_2 was set at 5.455×10^{-3}. Initial condition was chosen near stable P3-4. During $0 \le t < t_1$, β_2 is kept at 5.455×10^{-3}. The energy distribution, which has a peak between 3rd and 4th cantilevers, implies that the localized oscillation stands at P3-4. For $t_1 \le t < t_2$, β_2 decreases to 5.452×10^{-3}. Then P-modes lose the stability. As a result, the localized oscillation begins to leave P3-4. It quickly shifts to P4-5 through ST3 around $t = 2700$ and stays near P4-5 for a while. Then the transition occurs again and the localized oscillation reaches near P5-6. Here β_2 returns to 5.455×10^{-3} for $t_3 \le t < t_4$ and keeps its value during $t \ge t_4$. Since the P-modes are stabilized, the localized oscillation is caught near P5-6. Rigorously, it wanders around
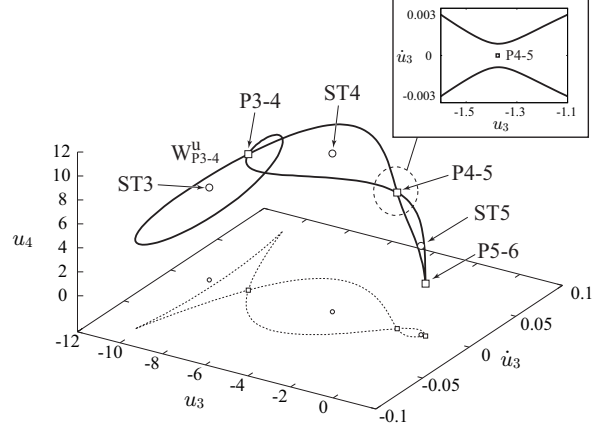

Figure 4: Unstable invariant manifold of P3-4 and some coexisting ILMs. They are on a hyper plane Σ_4. Solid-curve corresponds to unstable invariant manifold $W^{\mathrm{u}}_{\mathrm{P3-4}}$. Circle and square indicate stable and unstable ILMs, respectively. Projection to $(u_3, \dot{u}_3)$ plane is also drawn with dotted-curve and small points. Unstable manifold of right side extends to P5-6 and returns to P3-4 again. The opposite side one lies around ST3.

the stable P5-6. However it did not shift to another site beyond unstable ST-modes through the long time simulation. Consequently, it is shown that the localized oscillation can be moved from P3-4 to P5-6 by slightly varying β_2. In addition, the localization of energy distribution is held under the manipulation.

5. Concluding Remarks

In this paper, the stability and the transition of ILM in the cantilever array has been discussed based on the results of traveling waves in coupled magneto-elastic beam system. First, coexistence of ILMs was confirmed and the stability was investigated. ST-modes and P-modes coexist at every site except near the edges of the cantilever array. Their stability is changed by small change of the coefficient of nonlinear inter-site potential.

Second, an unstable manifold of P-mode was obtained and the phase structure was discussed. The unstable manifold passes by P-modes and takes a long way around ST-modes.

Finally, it was shown that the localized oscillation can be shifted to another site by appropriate modification of the nonlinear inter-site potential. The localized oscillation generated near a stable ILM begins to move when the ILM becomes unstable. The localization of energy distribution in space is kept while the oscillation moves. The moving localized oscillation is caught by the stable ILM. It should be noted that the place where the moving localized oscillation temporarily stay is decided by the structure of the invariant manifolds of unstable ILMs. The localized oscillation generated near a P-mode will not shift to any ST-modes.
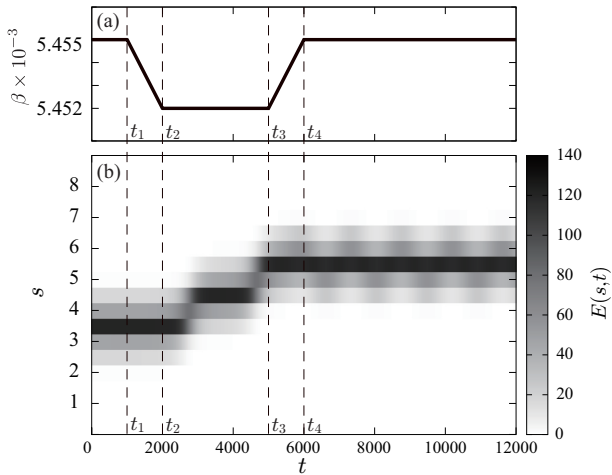
Figure 5: Transition of ILM via stability change. (a) Variation of β_2 with respect to time. β_2 decreases monotonously from 5.455×10^{-3} to 5.452×10^{-3} for $t_1 < t < t_2$. β_2 begins to return at $t = t_3$, It keeps 5.455×10^{-3} after $t = t_4$. (b) Energy distribution. Tone is related to energy density. Thus the most dark region corresponds to center of localized oscillation. At first, the oscillation stands between 3rd and 4th sites. It begins to move when P3-4 becomes unstable. Finally, the localized oscillation is stopped between 5th and 6th sites according to the stability of P3-4 changes again. As a result, the position of the localized oscillation is shifted from P3-4 to P5-6.

Acknowledgments

References

[1] A. J. Sievers and S. Takeno, "Intrinsic localized modes in anharmonic crystals," *Phys. Rev. Lett.*, vol.61, p.970, 1988.

[2] E. Trías, J. J. Mazo, and T. P. Orlando, "Discrete breathers in nonlinear lattices: Experimental detection in a josephson array," *Phys. Rev. Lett.*, vol.84, p.741, 2000.

[3] P. Binder, D. Abraimov, A. V. Ustinov, S. Flach, and Y. Zolotaryuk, "Observation of breathers in josephson ladders," *Phys. Rev. Lett.*, vol.84, p.745, 2000.

[4] A. V. Ustinov, "Imaging of discrete breathers," *Chaos*, vol.13, p.716, 2003.

[5] H. S. Eisenberg, Y. Silberberg, R. Morandotti, A. R. Boyd, and J. S. Aitchison, "Discrete spatial optical solitons in waveguide arrays," *Phys. Rev. Lett.*, vol.81, p.3383, 1998.

[6] R. Morandotti, U. Peschel, J. S. Aitchison, H. S. Eisenberg, and Y. Silberberg, "Dynamics of discrete solitons in optical waveguide arrays," *Phys. Rev. Lett.*, vol.83, p.2726, 1999.

[7] M. Sato, B. E. Hubbard, A. J. Sievers, B. Ilic, D. A. Czaplewski, and H. G. Craighead, "Observation of locked intrinsic localized vibrational modes in a micromechanical oscillator array," *Phys. Rev. Lett.*, vol.90, p.044102, 2003.

[8] David K. Campbell, Sergej Flach, and Yuri S. Kivshar, "Localizing energy through nonlinearity and discreteness," *Phys. Today*, vol.57, p.43, 2004.

[9] M. Sato, B. E. Hubbard, L. Q. English, A.J.Sievers, B. Ilic, D. A. Czaplewski, and H. G. Craighead, "Study of intrinsic localized vibrational modes in micromechanical oscillator arrays," *Chaos*, vol.13, p.702, 2003.

[10] M. Sato, B. E. Hubbard, and A. J. Sievers, "*Colloquium:* Nonlinear energy localization and its manipulation in micromechanical oscillator arrays," *Rev. Mod. Phys.*, vol.78, p.137, 2006.

[11] M. Sato, B. E. Hubbard, A. J. Sievers, B. Ilic, and H. G. Craighead, "Optical manipulation of intrinsic localized vibrational energy in cantilever arrays," *Europhys. Lett.*, vol.66, (3) p.318, 2004.

[12] T. Hikihara, Y. Okamoto, and Y. Ueda, "An experimental spatio-temporal state transition of coupled magneto-elastic system," *Chaos*, vol.7, p.810, 1997.

[13] T. Hikihara, K. Torii, and Y. Ueda, "Quasi-periodic wave and its bifurcation in coupled magneto-elastic beam system," *Phys. Lett. A*, vol.281, p.155, 2001.

[14] T. Hikihara, K. Torii, and Y. Ueda, "Wave and basin structure in spatially coupled magneto-elastic beam system − transitions between coexisting wave solutions," *Int. J. Bifurcat. and Chaos*, vol.11, p.999, 2001.

[15] S. Flach and A. Gorbach, "Discrete breathers in Fermi-Pasta-Ulam lattices," *Chaos*, vol.15, p.15112, 2005.

[16] J. B. Page, "Asymptotic solutions for localized vibrational modes in strongly anharmonic periodic systems," *Phys. Rev. B*, vol.41, p.7835, 1990.

[17] S. Flach and C. R. Willis, "Discrete breathers," *Phys. Rep.*, vol.295, p.181, 1998.